NATURAL CONVECTION FLOW ON A VERTICAL CYLINDER WITH SINUSOIDAL TEMPERATURE OSCILLATION UNDER THE EFFECT OF MAGNETO HYDRODYNAMIC

Asst. Prof. Manal H. AL-Hafidh

University of Baghdad / College of Engineering

Mech. Engr. Dept

ABSTRACT

The present work investigates the effect of magneto hydrodynamic (MHD) laminar natural convection flow on a vertical cylinder subjected to sinusoidal temperature oscillation. The governing equations which used are continuity, momentum and energy equations. These equations are transformed to dimensionless equations using vortices-stream function method and the resulting nonlinear system of partial differential equations are then solved numerically using finite difference approximation. A computer program was built to calculate the rate of heat transfer in terms of average Nussle number, velocity distribution as well as temperature distribution for a selection of magneto hydrodynamic parameter range $(0 \le M \le 10)$, dimensionless amplitude $(0 \le a \le 0.8)$ and dimensionless time τ' (0.2 – 0.8). Numerical solution have been considered for a fluid Prenatal
542 number fixed at (Pr=0.7), Rayleigh number $(1 \le Ra_l \le 10^4)$. Generally, the results show that Nu increase as Ra, M and a increase and decrease with τ'. The effect of Ra and M on the rate of heat transfer is concluded by a correlation. The results are found to be in good agreement compared with the results of **[**Adams, 1954**]** for the case of no MHD.

KEY WORDS: Natural convection, magneto hydrodynamic, sinusoidal oscillation, vertical cylinder .

الجريان بالحمل الطبيعي على أسطوانة عمودية بتذبذب جيبي في درجة الحرارة تحت تأثير الهيدروديناميكية المغناطيسية

د.منال هادي الحافظ
قسم الهندسة الميكانيكية / كلية الهندسة / جامعة بغداد

الخلاصة

تمت دراسة تأثير الهيدروديناميكية المغناطيسية على الحمل الحر للجريان الطباقي على اسطوانة عمودية خاضعة لتغير درجة الحرارة بتذبذب جيبي. المعادلات الحاكمة هي الاستمرارية والزخم والطاقة والتي تم تحويلها

الى معادلات لابعدية باستخدام دالة الانسياب الدوامية وتم حل المعادلات التفاضلية الجزئية اللاخطيّة عدديا باستخدام طريقة الفروق المحددة. تم بناء البرنامج الحاسوبي (Fortran 90) لحساب معدل انتقال الطاقة الحرارية بدلالة معدل عدد نسلت وتوزيع السرعة ودرجة الحرارة للمعايير التي تتضمن مجموعة من القيم الابعدية المتمثلة بالهيدروديناميكية المغناطيسية $(0.0 \le M \le 1.0)$ والسِعة اللابعدية $(0 \le a \le 0.8)$ والزمن اللابعدي τ' (0.2–0.8) والاخذ بنظر الاعتبار الحل العددي لمائع ذو عدد براندتل (Pr=0.7) وعدد رايلي $(1 \le Ra_l \le 10^4)$. بيّنت النتائج أن عدد نسلت يزداد بزيادة Ra و M و a ويقل بزيادة τ'. النتائج أعطت تمثيل لعدد نسلت ضد Ra و M. المقارنة مع البحوث الأخرى أعطت نتائج دقيقة كفاية بالمقارنة مع نتائج [Adams, 1954] في حالة عدم وجود تأثير الهيدروديناميكية المغناطيسيةM .

INTRODUCTION

The effects of buoyancy on steady-periodic flows are not so widely investigated and on the contrary unsteady boundary conditions compatible with a steady-periodic regime have been widely studied with reference to forced convection flows. The problem of natural convection due to a heated or cooled vertical cylinder provides one of the most basic scenarios for heat transfer theory and thus is of considerable theoretical and practical interest. The natural convection boundary-layer over a vertical cylinder is probably the first buoyancy convective problem which has been studied and it has been a very popular research topic for many years**.**

Magneto hydrodynamics is motivated by its widespread application to the description of space within the solar system (as taken in this study) and astrophysical plasmas (beyond the solar system).

[Kwak et al., 1998**]** Show that, for wall temperature oscillations having sufficiently high amplitude, there exists a critical frequency which corresponds to a maximum of the time averaged heat flux.

[Barletta et al., 2004] Investigated mixed convection flow in a vertical circular duct subjected to a periodic sinusoidal temperature change at the wall. The analysis was performed by considering fully-developed parallel flow and steady-periodic regime. Two independent boundary value problems considered which provide the mean value and the oscillating term of the velocity and temperature distributions. These boundary value problems are solved analytically, and the velocity and temperature distributions were obtained as functions of three parameters: the Prenatal number, (Pr), the dimensionless frequency (X), the ratio between the Grashof number Gr and the Reynolds number (Re).

[Molla1 and Taher1, 2005**]** study the effect of magneto hydrodynamic natural convection flow on a sphere in present of heat generation. Results indicated that the local Nussle no. (Nu_x) decreases owing to increase the value of heat generation (Q) and the local rate of heat transfer Nu_x decreased slightly as the value of magnetic parameter M increased at different positions. The velocity distribution decreased slightly as the magnetic parameter (M) increased, but near the surface of the sphere velocity increased and became maximum and then decreased and finally approached to zero.

[Filar, Fernlike and Knead, 2005**]** Investigated numerically three-dimensional convection of air inside a vertical cylinder isothermally heated and cooled from a side Wall for both magnetic and gravity fields. A single electric coil was placed around the cylinder to generate a magnetic field. Convection was calculated for various coil level

and magnetic strengths. The results indicated that effect of Magneto hydrodynamic increased and cause to increase the rate of heat transfer and this is clear at higher values of Rayleigh number and both coil elevation and Rayleigh number affect the heat transfer rate extensively. The maximum Nussle number could be obtained for the coil located at about half of cylinder.

[Kandaswamy et al., 2008**]** Magneto convection of an electrically conducting fluid in a square cavity with partially thermally active vertical walls was investigated numerically. The active part of the left side wall was at a higher temperature than the active part of the right side wall. The top, bottom and the inactive parts of the side walls are thermally inactive. Nine different combinations of the relative positions of the active zones were considered. The results show that heat transfer rate is maximum for the middle–middle thermally active locations while it is poor for the top–bottom thermally active locations. The average Nusselt number decreases with an increase of Hartmann number and increases with an increase of Grashof number. For sufficiently large magnetic field Ha = 100 the convective mode of heat transfer is converted into conductive mode in the low region of Grashof number than in the high region.

A series of numerical simulations were performed by **[**Kakarantzas et al., 2009] in order to study liquid metal MHD natural convection in a vertical cylindrical container with a sinusoidal temperature distribution at the upper wall and the other surfaces being adiabatic. Starting from the basic hydrodynamic case, the effect of vertical (axial) and horizontal magnetic fields is assessed. Depending on the magnitude of the Rayleigh and Hartmann numbers, both turbulent and laminar (azimuthally symmetric or not) flows are observed. The results show that the increase of Rayleigh number promotes heat transfer by convection while the increase of Hartmann number favors heat conduction. The vertical magnetic field reduces the Nusselt number more than the horizontal. The circulation patterns for the most convective cases are confined close to the top corner of the container with the simultaneous formation of a secondary flow pattern at the bottom corner, while for the more conductive cases only one circulation pattern exists covering the entire domain.

[Pirmohammadi et al., 2010**]** Investigated numerically magneto hydrodynamics natural convection in an inclined partitioned enclosure. The vertical walls were maintained isothermal at different temperatures and other walls were adiabatic. Two insulated partitions were located on horizontal walls. Non linear governing equations for the fluid flow and heat transfer were solved for different inclination angle, Hartmann numbers and partition heights H_p. It was found as H_p non dimensional and Hartmann number (Ha) increase the mean Nusselt number decreases. Also the variation of mean Nusselt number with inclination angle in low Hartmann number is more considerable compare to high Hartmann number. In the present study, the magneto hydrodynamic, effect was investigated for steady state laminar natural convection external flow on a vertical cylinder, for thermal boundary condition of sinusoidal temperature oscillation at all walls and for ($1 \leq Ra_l \leq 10^4$) and magneto hydrodynamics ($0 \leq M \leq 10$).

MATHEMATICAL MODEL

The mathematical modeling will be set for laminar natural convection heat transfer on a vertical cylinder. The buoyancy effect caused by the density variation produces Natural circulation resulting in the fluid motion relative to the bounding solid surface. The buoyancy forces behave as body forces and are included as such in the momentum equation. Under these conditions the continuity, momentum and energy equations are coupled.

The density is considered as linear function of temperature so that the usual Boussinesq's approximation is taken as **[**Singh and Kumar**,** 2003**]**:

$$\rho = \rho_o \left(1 - \beta \left[T - T_\infty \right] \right) \tag{1}$$

$$g_r = 0 \tag{2}$$

$$g_z = g\beta(T - T_\infty) \tag{3}$$

Continuity Equation

The equation of conservation of mass in the cylindrical coordinates is given as **[**Herman, 1978**]**:

$$\frac{1}{r}\frac{\partial}{\partial r}(r\,u) + \frac{\partial w}{\partial z} = 0 \tag{4}$$

Momentum Equation

By using Navier-Stokes' equation in the cylindrical coordinates (r, z), the equation of conservation of momentum in the cylindrical coordinates (the radial (r) direction) is in the following form **[**Herman, 1978**]**:

$$u\frac{\partial u}{\partial r} + w\frac{\partial u}{\partial z} = -\frac{1}{\rho}\frac{\partial P^*}{\partial r} + \nu\left(\frac{\partial}{\partial r}\left[\frac{1}{r}\frac{\partial}{\partial r}(ru) \right] + \frac{\partial^2 u}{\partial z^2} \right) + f_r \tag{5}$$

Where (f_r) is the electromagnetic force in (r) direction **[**Herman **,** 1978**]**:

$$f_r = \frac{\sigma_o B_o^2 u}{\rho} \tag{6}$$

The equation of conservation of momentum in the cylindrical coordinates (in the axial (z) direction) is in the following form:

$$u\frac{\partial w}{\partial r} + w\frac{\partial w}{\partial z} = -\frac{1}{\rho}\frac{\partial P^*}{\partial z} + \nu\left(\frac{1}{r}\frac{\partial}{\partial r}\left[r\frac{\partial w}{\partial r} \right] + \frac{\partial^2 w}{\partial z^2} \right) + g\beta(T - T_\infty) + f_z \tag{7}$$

Where (f_z) is the electromagnetic force in (z) direction **[**Herman **,** 1978**]**:

$$f_z = \frac{\sigma_o B_o^2 w}{\rho}$$

Energy Equation

The energy equation in the cylindrical coordinates takes the following form:

$$u\frac{\partial T}{\partial r}+w\frac{\partial T}{\partial z}=\alpha\left(\frac{1}{r}\frac{\partial}{\partial r}\left[r\frac{\partial T}{\partial r}\right]+\frac{\partial^2 T}{\partial z^2}\right) \qquad (8)$$

DIMENSIONLESS PARAMETERS AND EQUATIONS

$$\left(R=\frac{r}{l}\right),\quad \left(Z=\frac{z}{l}\right),\quad \left(U=\frac{u\,l}{\alpha}\right),\quad \left(W=\frac{\mathrm{w}l}{\alpha}\right),\quad \left(\theta=\frac{T-T_\infty}{T_w-T_\infty}\right),$$

$$\left(P=\frac{pl^2}{\rho\alpha^2}\right)\quad \left(M=\frac{\sigma_\circ B_\circ^2 l^2}{\rho\alpha}\right)$$

Dimensionless Continuity Equation

$$\frac{1}{R}\frac{\partial(RU)}{\partial R}+\frac{\partial W}{\partial Z}=0 \qquad (9)$$

Dimensionless Momentum Equation In (r) Direction

$$U\frac{\partial U}{\partial R}+W\frac{\partial U}{\partial Z}=-\frac{\partial P}{\partial R}+\mathrm{Pr}\left(\frac{\partial}{\partial R}\left(\frac{1}{R}\frac{\partial(RU)}{\partial R}\right)+\frac{\partial^2 W}{\partial Z^2}\right)+MU \qquad (10)$$

Dimensionless Momentum Equation In (z) Direction

$$U\frac{\partial W}{\partial R}+W\frac{\partial W}{\partial Z}=-\frac{\partial P}{\partial Z}+\mathrm{Pr}\left(\frac{1}{R}\frac{\partial}{\partial R}\left(R\frac{\partial W}{\partial R}\right)+\frac{\partial^2 W}{\partial Z^2}\right)+\mathrm{Pr}\,Ra_l\,\theta+MW \qquad (11)$$

Dimensionless Energy Equation

$$U\frac{\partial\theta}{\partial R}+W\frac{\partial\theta}{\partial Z}=\left[\frac{1}{R}\frac{\partial}{\partial R}\left(R\frac{\partial\theta}{\partial R}\right)\right]+\frac{\partial^2\theta}{\partial Z^2} \qquad (12)$$

Vorticity Transport, Stream Function and Energy Equation

The governing equations in dimensionless form above were written in terms of dependant variables (U, W, P and θ). It may be recommended to eliminate pressure term (because it will be a non linear term in momentum equation) **[**Patanker, 1980**]**.

By converting momentum equations to vorticity transport equation by differentiate momentum equation in (r) direction with respect to (z) and momentum equation in (z) direction with respect to (r) and subtract them from each other and make use of continuity equation and vorticity definition:

$$\omega = \frac{\partial W}{\partial R} - \frac{\partial U}{\partial Z} \tag{13}$$

$$\frac{\partial (U\omega)}{\partial R} + \frac{\partial (W\omega)}{\partial Z} = \Pr Ra_1 \frac{\partial \theta}{\partial R} + M\omega + \Pr\left(\frac{\partial}{\partial R}\left(\frac{1}{R}\frac{\partial (R\omega)}{\partial R} \right) + \frac{\partial^2 \omega}{\partial Z^2} \right) \tag{14}$$

Also, by making use of vorticity definition (15) and the definition of stream function, (ψ) which satisfy continuity equation, the vertical and radial velocities can be written as follows respectively:

$$W = -\frac{1}{R}\frac{\partial \psi}{\partial R} \tag{15}$$

$$U = \frac{1}{R}\frac{\partial \psi}{\partial Z} \tag{16}$$

So by substituting the velocity components (15) and (16) in vorticity definition equation (13), stream function equation resulted as:

$$-\omega = \frac{1}{R}\left(\frac{\partial^2 \psi}{\partial R^2} - \frac{1}{R}\frac{\partial \psi}{\partial R} + \frac{\partial^2 \psi}{\partial Z^2} \right) = \nabla^2 \psi \tag{17}$$

The dimensionless energy equation (12) can be transformed to another form by substituting the continuity equation (9) in it as follows:

$$\frac{1}{R}\frac{\partial (RU\theta)}{\partial R} + \frac{\partial (W\theta)}{\partial Z} = \left[\frac{1}{R}\frac{\partial}{\partial R}\left(R\frac{\partial \theta}{\partial R} \right) \right] + \frac{\partial^2 \theta}{\partial Z^2} \tag{18}$$

Boundary Conditions;

The imposed boundary conditions (illustrate in **Fig. (1)** and **Table (1)**), rewritten in terms of stream function and vorticity

$\omega = \psi = U = W = 0$ (no slip condition)

$\theta = 1$ (constant wall temperatures for a=0)

$\theta = 1 +$ a sin $(2\pi\tau/\acute{\eta})$ (sinusoidal oscillation temperature)

[Barletta et al., 2004]

NUMERICAL SOLUTION

The method of the numerical solution taken is the Finite Difference technique for solving the set of equations **[**Patanker, 1980**]**.

$$a_1\theta_{i-1,j} + a_2\theta_{i+1,j} + a_3\theta_{i,j} + a_4\theta_{i,j-1} + a_5\theta_{i,j+1} = 0 \quad (19)$$

Where:

$$a_1 = \frac{(U_b + |U_b|)(\Delta R(1-2i) - R_i)}{4\Delta R(R_i + i\Delta R)} + (-\frac{1}{(\Delta R)^2} + \frac{1}{2\Delta R(R_i + \Delta R)}) \quad (20)$$

$$a_2 = \frac{(U_f - |U_f|)(R_i + \Delta R(1+2i))}{4\Delta R(R_i + i\Delta R)} - (\frac{1}{\Delta R^2} + \frac{1}{2\Delta R(R_i + \Delta R)}) \quad (21)$$

$$a_3 = \frac{[(U_f + |U_f|)(R_i + \Delta R(1+2i)) + (U_b - |U_b|)(\Delta R(1-2i) - R_i)]}{4\Delta R(R_i + i\Delta R)} + \frac{(W_f + |W_f| - W_b + |W_b|)}{2\Delta Z} + \frac{2}{(\Delta R)^2} + \frac{2}{(\Delta Z)^2} \quad (22)$$

$$a_4 = \frac{(-W_b + |W_b|)}{2\Delta Z} - \frac{1}{(\Delta Z)^2} \quad (23)$$

$$a_5 = \frac{(W_f - |W_f|)}{2\Delta Z} - \frac{1}{(\Delta Z)^2} \quad (24)$$

$$b_1\omega_{i-1,j} + b_2\omega_{i+1,j} + b_3\omega_{i,j} + b_4\omega_{i,j-1} + b_5\omega_{i,j+1} + c = 0 \quad (25)$$

Where:

$$b_1 = -\frac{(U_b + |U_b|)}{2\Delta R} + \frac{1}{2\Delta R(R_i + i\Delta R)} - \frac{1}{(\Delta R)^2} \quad (26)$$

$$b_2 = \frac{(|U_f| - U_f)}{2\Delta R} - \frac{1}{2\Delta R(R_i + i\Delta R)} - \frac{1}{(\Delta R)^2} \quad (27)$$

$$b_3 = -M + \frac{\left[\left(U_f + |U_f|\right) - \left(U_b + |U_b|\right)\right]}{2\Delta R} + \frac{\left(W_f + |W_f| - W_b + |W_b|\right)}{2\Delta Z} + \frac{2\,\mathrm{Pr}}{(\Delta R)^2} + \frac{2\,\mathrm{Pr}}{(\Delta Z)^2} + \frac{\mathrm{Pr}}{(R_I + i\Delta R)^2}$$

(28)

$$b_4 = -\frac{\left(W_b + |W_b|\right)}{2\Delta Z} - \frac{\mathrm{Pr}}{(\Delta Z)^2} \tag{29}$$

$$b_5 = \frac{\left(W_f - |W_f|\right)}{2\Delta Z} + \frac{\mathrm{Pr}}{(\Delta Z)^2} \tag{30}$$

$$c = -\frac{\mathrm{Pr}\,Ra\left(\theta_{i+1,j} - \theta_{i-1,j}\right)}{2\Delta R} \tag{31}$$

$$\psi_{i,j}^{\,it+1} = (1-\Omega)\psi_{i,j}^{\,it} + \frac{\Omega}{4}\left[\begin{array}{l}(R_i + i\Delta R)(\Delta R)^2\,\omega'_{i,j} + \left(\frac{R_i + \Delta R(i-0.5)}{(R_i + i\Delta R)}\right)\psi_{i+1,j}^{\,it} \\ \left(\frac{R_i + \Delta R(i+0.5)}{(R_i + i\Delta R)}\right)\psi_{I-1,J}^{\,it+1} + \left(\psi_{i,j+1}^{\,it+1} + \psi_{i,j-1}^{\,it+1}\right)\end{array}\right] \tag{32}$$

Where the parameter (Ω) is the over relaxation coefficient and its value is $(1 \le \Omega \le 1.5)$.

The local Nusselt number at the heated wall:

$$Nu_l = -\left(\frac{\partial\theta}{\partial R}\right) \tag{33}$$

The average Nusselt number along a single channel wall is defined by**[**Schwab and De Witt, 1970**]**:

$$N\bar{u} = -\frac{1}{l}\int_0^l Nu\; dZ \tag{34}$$

RESULTS AND DISCUSION

Effect of Different Parameters on Heat Transfer

Streamlines and Isotherms.

Fig. (2) and Fig. (3) Show the streamlines and isotherms for different values of Ra_l with constant temperature and with no magneto hydrodynamic. The mechanism of the flow occurs when the fluid near the hot wall is heated causing the density to be decreased and the fluid will be start to move upward nearby the hot wall towards the cold wall. It can be seen that the values of streamlines and isotherms at the cylinder surface increased when Ra_l increased. The isotherms will be closer to the cylinder and its value decreased from the surface to the ambient as Ra_l increased.

Fig. (4) and **Fig.(5)** show the effect of the dimensionless amplitude (a) for different values of Ra_l and with no magneto hydrodynamic. It is clear that the increase of (a) cause a very slight increase in Nu while increasing Ra_l cause a distinct increase in the values of streamlines and a wide region of temperature distribution in the lateral direction for Ra_l (10^2) but for higher Ra_l the region of temperature distribution will be decreased because the convection mode will be the dominant and heat transfer increase due to this which cause the streamlines to be closer to the cylinder.
A slight increase in streamlines and isotherms are shown in **Figs. (6-9)** when M increases for different values of Ra_l and a. The flow exhibits a simple circulating pattern rising along the hot wall and descending along the cold wall of the cavity. It is interesting to note that as the strength of the magnetic field increases the central streamlines are elongated horizontally and the temperature stratification in the core diminishes. The isotherms are almost parallel and are nearly conduction like and this is due to the suppression of convection by the magnetic field. For higher Rayleigh number and low M, the thermal boundary layers are well established along the side
Walls and the temperature stratification exists. This is because convection is the dominant mode of heat transfer at high Rayleigh number. From these figures, it is also observed that for higher Rayleigh number the effect of M on the temperature distribution is not prominent compared to that in the case of small Ra_l.

The Variation of Average Nu with Ra_l.

The variation of the average Nusselt number Nu with Ra_l is shown in **Fig. (10)** For different values of M. The increase in Nu when the effect of M is included is clear for $Ra_l = 10^2$ and the effect decrease until $Ra > 10^4$ then curves coincides.

The Effect of M on Nu Including Other Parameters

Fig.(11) and **Fig.(12)** show the variation of Nu with M for different values of (a) and Ra_l. When the dimensionless amplitude included the effect of M increased and cause to increase the rate of heat transfer and this is clear at higher values of Ra_l.

The Variation of Average Nu with Dimensionless amplitude and Dimensionless Time.

Fig.(13) and **Fig.(14)** illustrate that the variation of Nu is hardly affected by (a) or by the dimensionless time for a given value of Ra_l .

COMPARISON OF THE RESULTS

A comparison was done between the result of the present study for the variation of Nu with Ra_l and the correlation of **(Mc Adams, 1954)** which is shown in **Fig.(15)** with a deviation of 5% for the case of no M and a.
A correlation has been set up to give the average Nusselt number variation with Ra and M. This correlation is made by using the computer program (DGA v1.00).

$$Nu = 6.3215\ Ra_l^{2.998}\ M^{3.9065} \quad (35)$$

NOMENCLATUR
LATIN SYMBOLS

Symbol	Description	Unit
Cp	Specific heat at constant pressure	kJ/kg.K
f_r	Electromagnetic force in (r) direction	m/s^2
f_z	Electromagnetic force in (z) direction	m/s^2
g	Acceleration due to gravity	m/s^2
Gr	Grashof number $\left(Gr = \frac{g\beta(T_w - T_\infty)l^3}{\nu^2}\right)$	
h	Heat transfer coefficient	$W/m^2.^oC$
Ha	Hartmann number ($Ha^2=\frac{\sigma\beta_\circ^2 R^2}{\mu}$)	
i	R-direction directory	-
j	Z-direction directory	-
K	Thermal conductivity	$W/m.^oC$
K^*	Mean absorption coefficient	m^{-1}
l	Length of cylinder	m
M	Dimensionless Magneto hydrodynamic parameter	-
n	Indicate the unit vactor	m
N	Dimensionless Conduction-Radiation parameter	-
Nu	Average Nusselt number(Nu=hl/k)	-
P^*	Air pressure	N/m^2
P	Normalized air pressure	-
Pr	Prandtl number(Pr=ν/α)	-
q_r	Radiative heat flux	W
q	Overall heat transfer	W
Q	Dimensionless overall heat generation	-
Q_o	Heat generation/absorption	$W/m^3.^oC$
q'''	Volumetric heat generation	W/m^3
r	Radial direction	m
R	Dimensionless Radial direction	-
Ra_l	Rayleigh no. $\left(Ra_l = \frac{\Pr g\beta(T_w - T_\infty)l^3}{\nu^2}\right)$	-
T	Air temperature	K
T_∞	Ambient temperature	K
u	Radial velocity	m/s
U	Dimensionless Radial velocity	-
w	Vertical velocity	m/s
W	Dimensionless Vertical velocity	-
X	Nodes number in r-direction	-
Y	Nodes number in z-direction	-
z	Vertical direction	m
Z	Dimensionless Vertical direction	-

CREAK SYMBOLS

Symbol	Description	Unit
α	Thermal diffusivity	m^2/s
β	Coefficient of thermal expansion	K^{-1}
ε	Emissivity	-
θ	Dimensionless temperature	-
λ	Radii ratio	-
μ	Viscosity	kg/m.s
ν	Kinematic viscosity	m^2/s
ρ	Air density	kg/m^3
σ	Stefan-Boltzmann constant	$W/m^2.K^4$
ψ	Dimensionless stream function	-
ω	Dimensionless vorticity	-

Subscript

Symbol	Description	Unit
(i,j)	Grid nodes in (r,z) direction	-

Table (1) Boundary Conditions

Line	Θ	ψ	ω	W,U
AB	$\frac{\partial\theta}{\partial R}=0$	0.0	0.0	0.0
BC	1+ a sin (2πτ/ή)	0.0	$\omega=-\frac{1}{Z}\frac{\partial^2\psi}{\partial R^2}$	0.0
CD	1+ a sin (2πτ/ή)	0.0	$\omega=-\frac{1}{R}\frac{\partial^2\psi}{\partial Z^2}$	0.0
DE	1+ a sin (2πτ/ή)	0.0	$\omega=-\frac{1}{Z}\frac{\partial^2\psi}{\partial R^2}$	0.0
EF	$\frac{\partial\theta}{\partial R}=0$	0.0	0.0	0.0
FG	0.0	$\frac{\partial\psi}{\partial Z}=0$	0.0	0.0
GH	0.0	$\frac{\partial\psi}{\partial R}=0$	0.0	0.0
HA	$\frac{\partial\theta}{\partial Z}=0$	$\frac{\partial\psi}{\partial Z}=0$	0.0	0.0

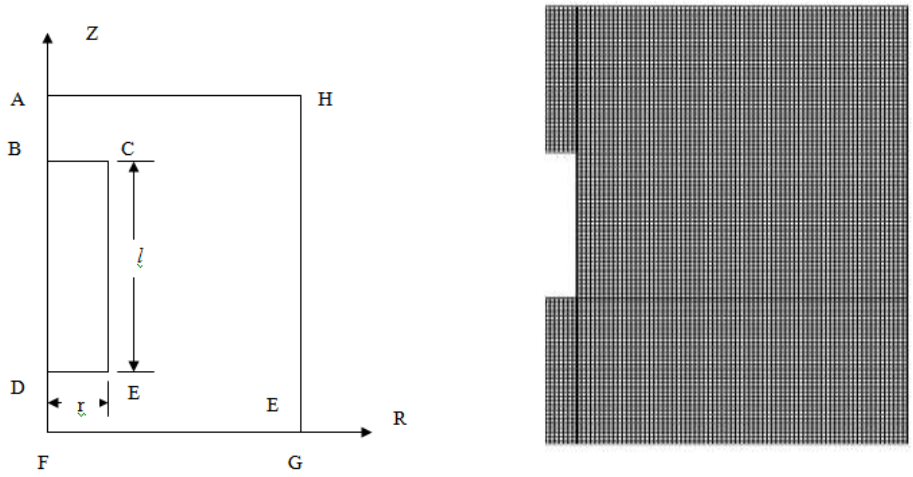

Fig. (1) The boundary condition and the grid of the problem

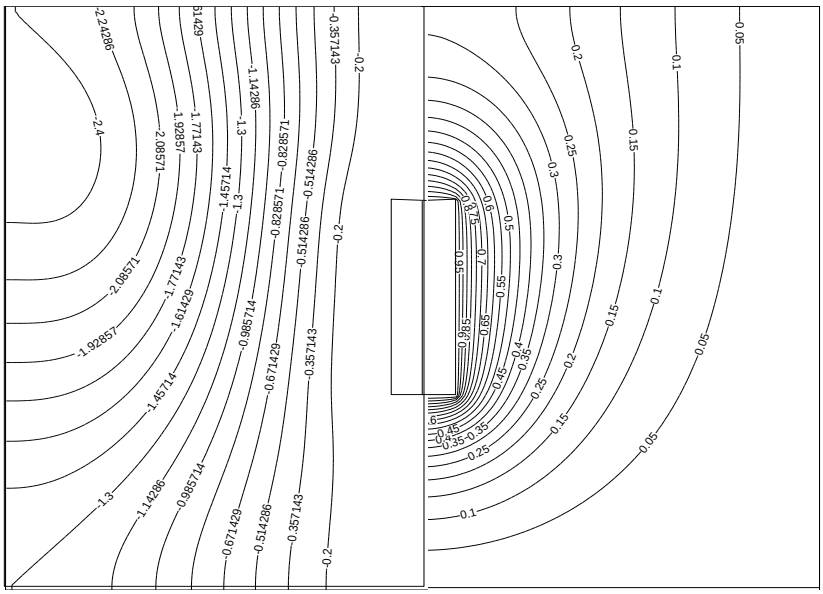

Streamlines **Isotherms**

Fig (2) Streamlines and isotherm for $Ra=10^2$, Mn=0, a=0

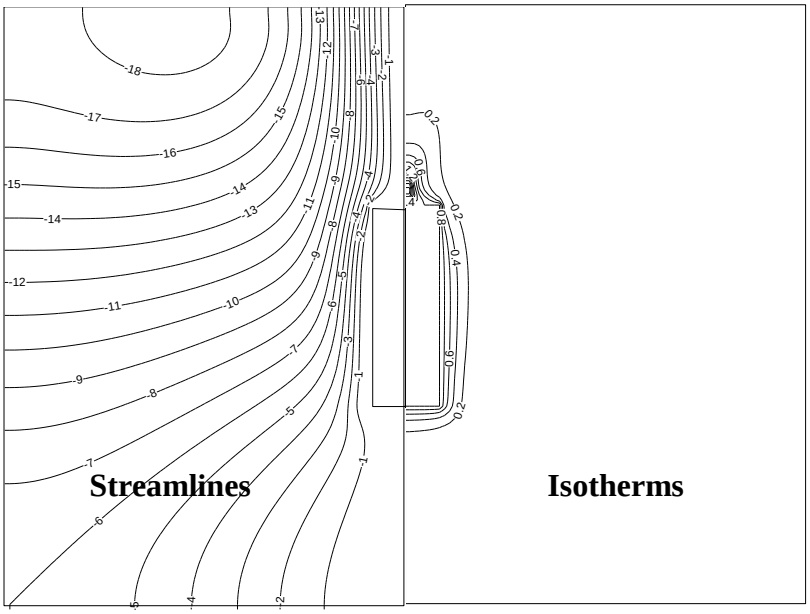

Fig (3) Streamlines and isotherm for $Ra=10^5$, Mn=0, a=0

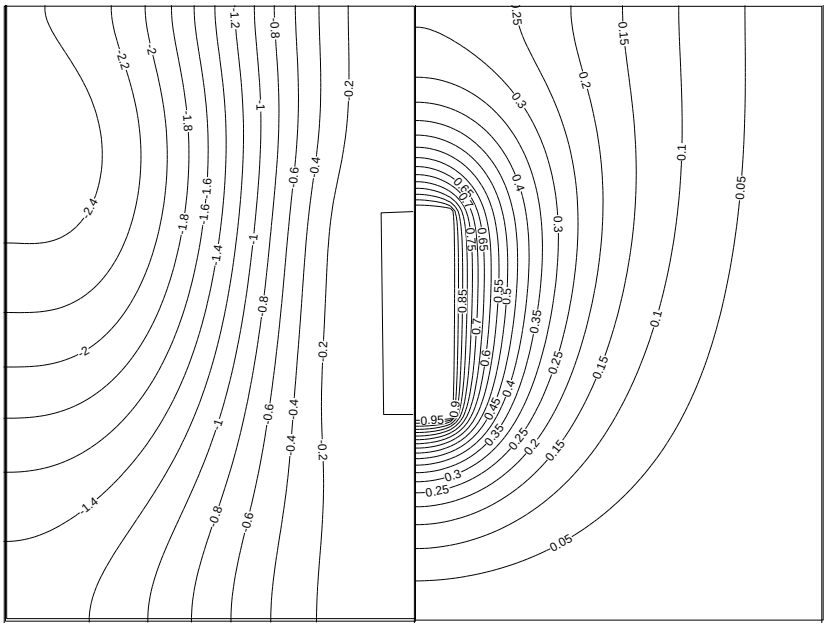

Fig (4) Streamlines and isotherm for $Ra=10^2$, Mn=0, a=0.8

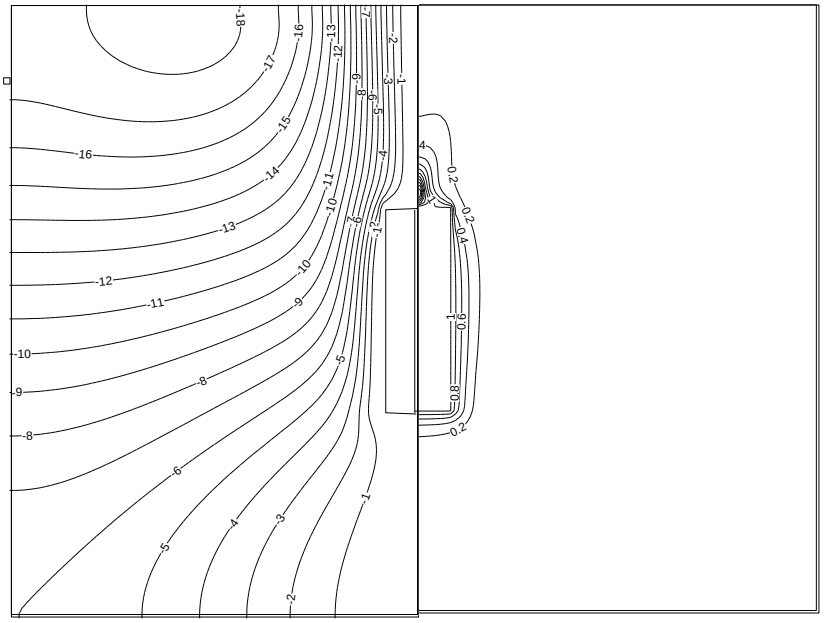

Streamlines **Isotherms**

Fig (5) Streamlines and isotherm for $Ra=10^5$, Mn=0, a=0.8

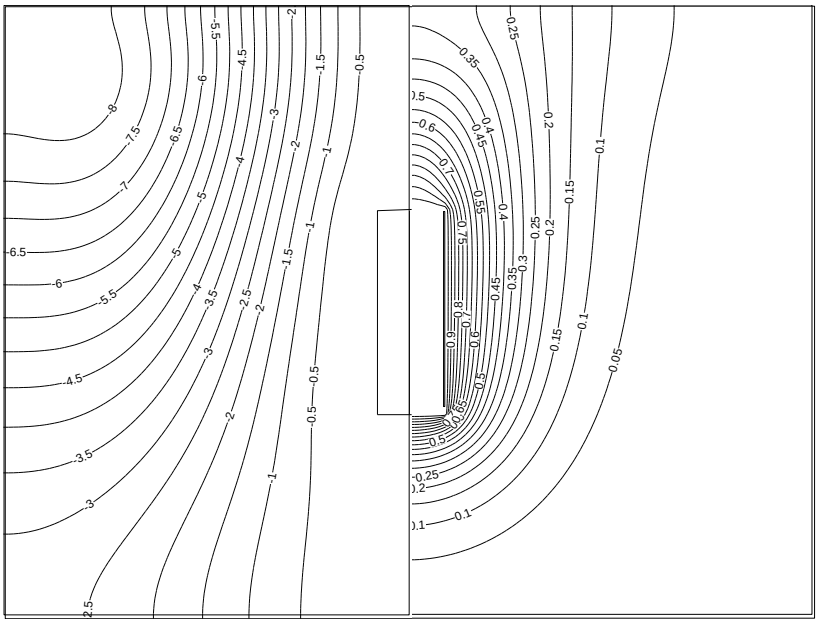

Streamlines **Isotherms**

Fig (6) Streamlines and isotherm for $Ra=10^2$, Mn=10,a=0

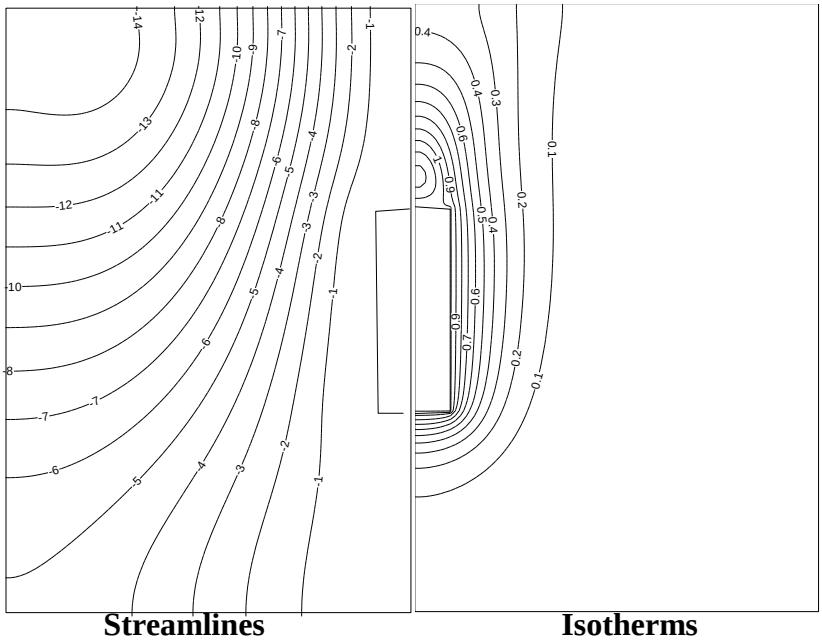

Streamlines **Isotherms**

Fig (7) Streamlines and isotherm for Ra=10^2 , Mn=10, a=0.8

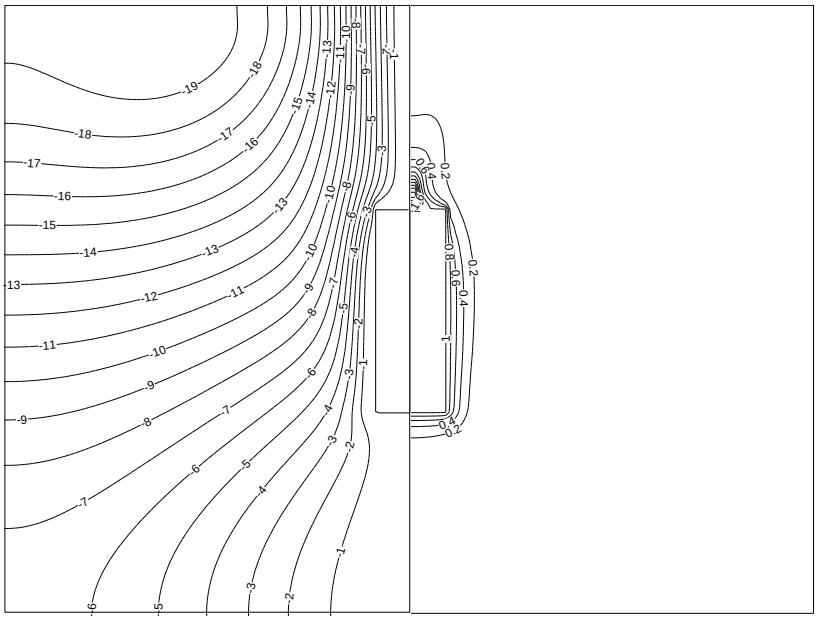

Streamlines **Isotherms**

Fig (8) Streamlines and isotherm for Ra=10^3 , Mn=10, a=0.8

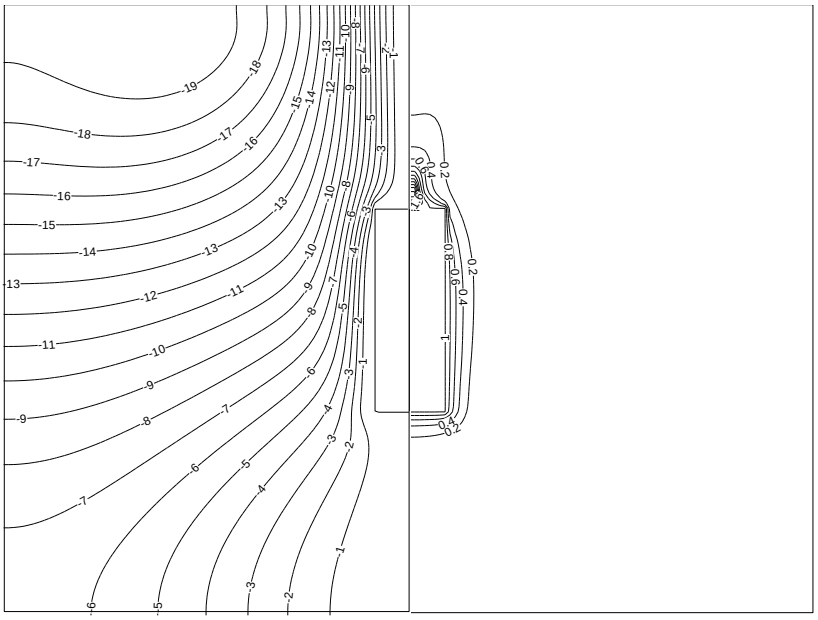

Streamlines **Isotherms**

Fig (9) Streamlines and isotherm for Ra=10^5 , Mn=10, a=0.8

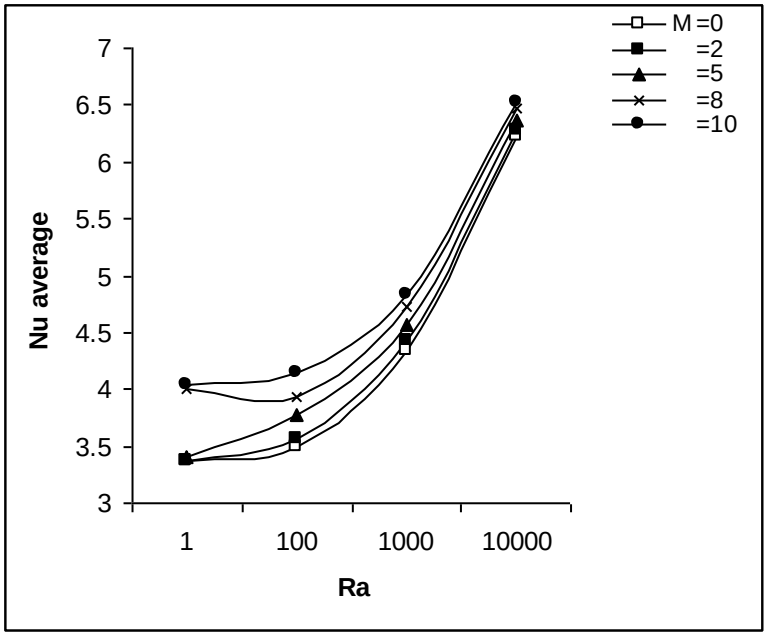

Fig (10) Variation of Nu with Ra for different values of M

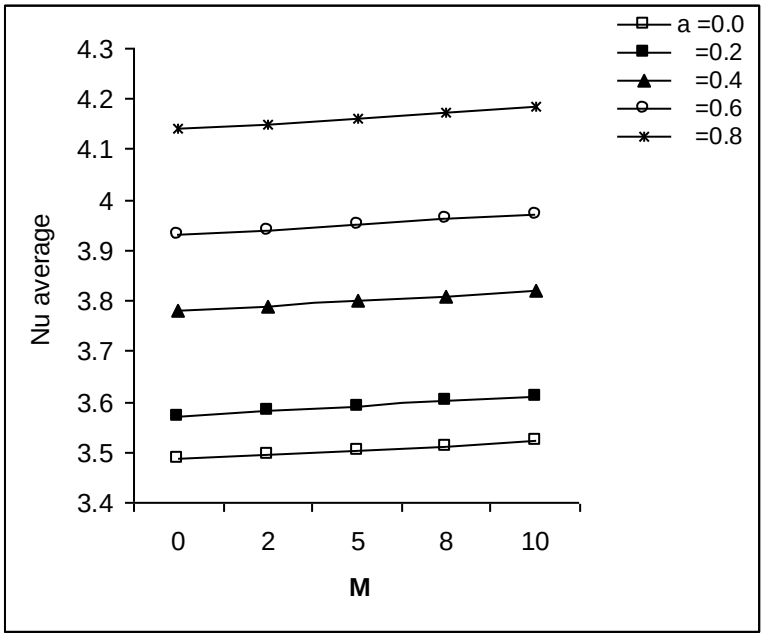

Fig (11) Variation of Nu with M for Ra= 10^2 and for different values of a

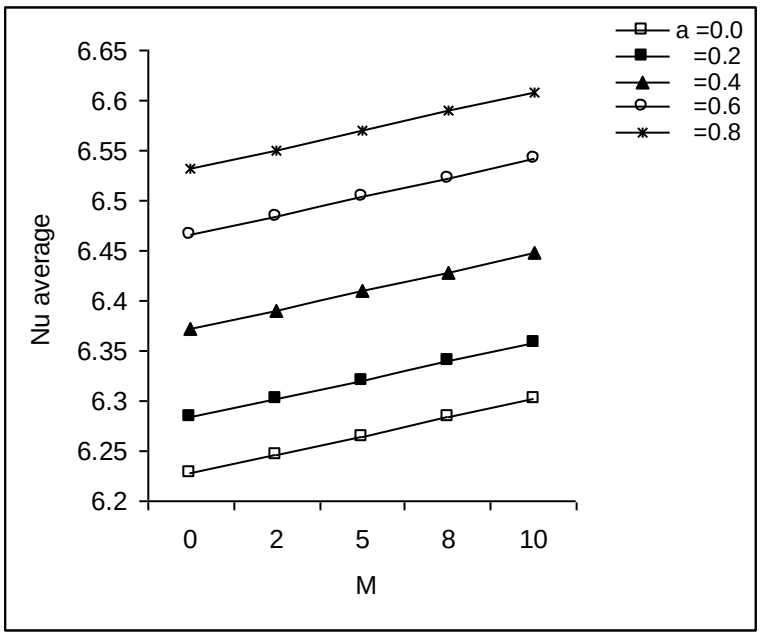

Fig (12) Variation of Nu with M for Ra= 10^4 and for different values of a

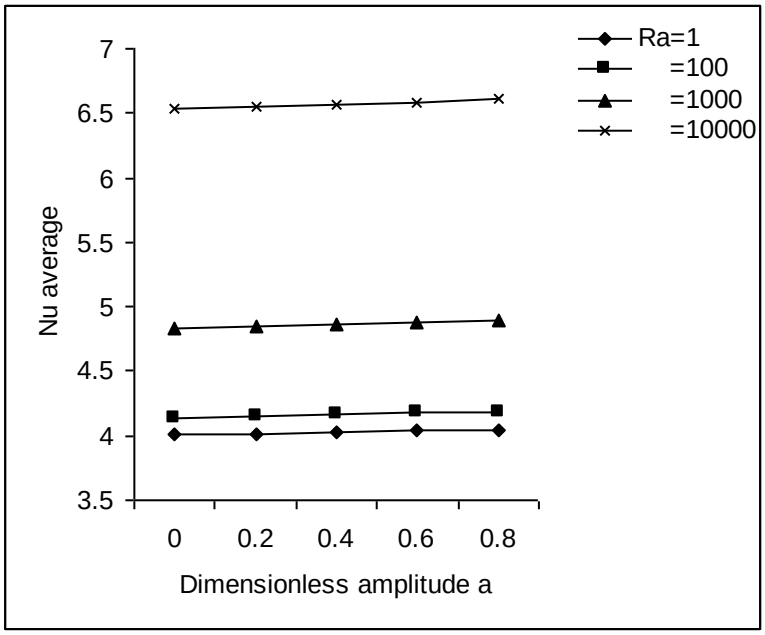

Fig (13) Variation of Nu with the dimensionless amplitude for M=10 and for different values of Ra

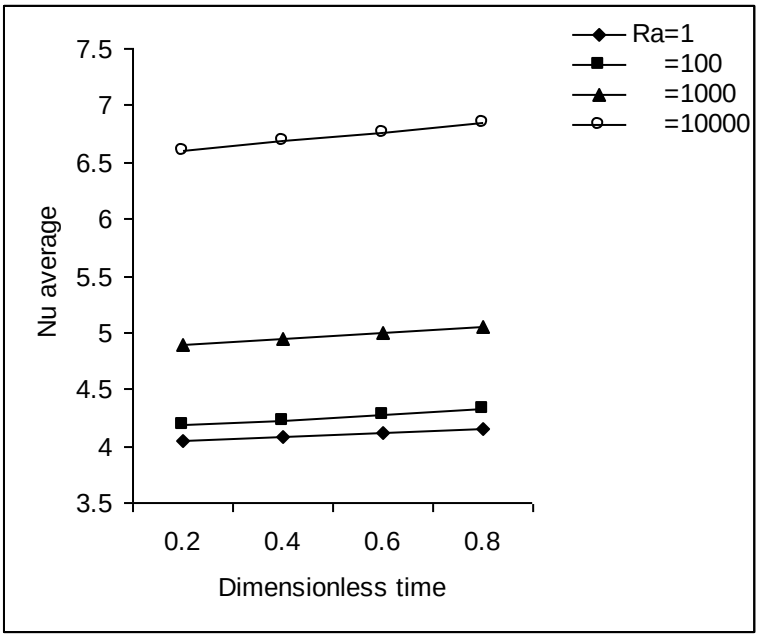

Fig (14) Variation of Nu with the dimensionless time for M=10 and for different values of Ra

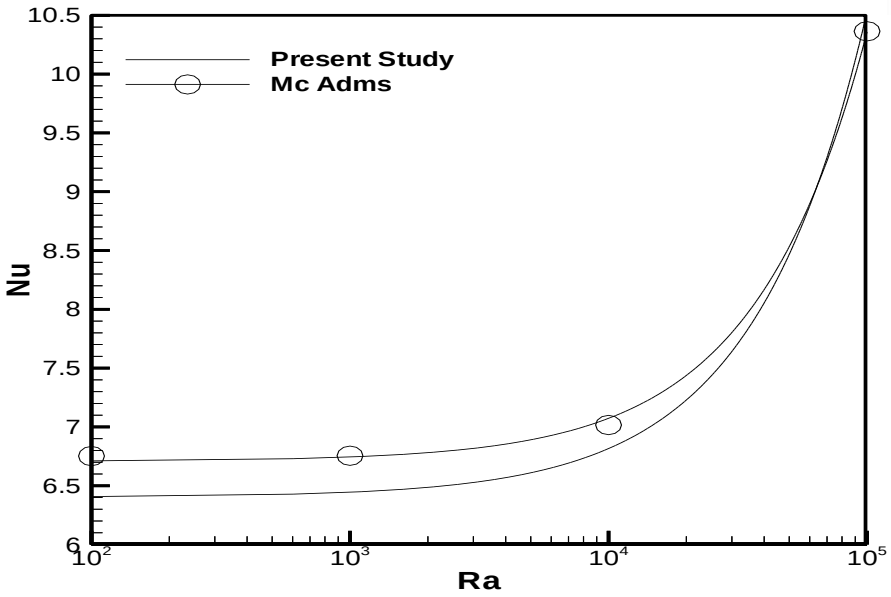

Fig (15) Comparison of the present study with [1]

CONCLUSIONS

From the present work results and for the cylinder that described previously, the following conclusions can be obtained:

1. A distinct increase in average Nu with increase in Ra_l.
2. Nu is hardly affected by the dimensionless amplitude and/or with the dimensionless time.
3. A clear increase in the average Nu when M included at low Ra_l this effect decrease until Ra_l exceed 10^4 then the effect vanish.

REFERENCES

[1] Adms Mc, W. H. , "Heat Transmission", 3d ed. McGrew-Hill Book Company, New York, (1954).
[2] Kwak H.S., Kuwahara K. and Hyun J.M., "Resonant enhancement of natural convection heat transfer in a square enclosure", Int. J. of Heat and Mass Transfer 41 (1998) 2837–2846.
[3] Barletta A. and Rossi di Schio E.,"Mixed convection flow in a vertical circular duct with time-periodic boundary conditions: steady-periodic regime", Int. J. of Heat and Mass Transfer 47 (2004) 3187–3195.
[4] Molla1 Md. M., Taher1 M.A., Chowdhury1 Md. M.K. and Hossain Md. A., "Magneto hydrodynamic Natural Convection Flow on a Sphere in Presence of Heat Generation ", Int. J. Heat and Mass Transfer. Vol. 10, No. 4 (2005) 349–363.
[5] Filar P., Fornalik E. and Kaneda M., "Three Dimensional Numerical Convection of Air Inside a Cylinder Heated and Cooled Isothermally from a Side Wall", Int. J. Heat and Mass Transfer. 48 (2005) 1858-1867.

[6] Kandaswamy P., Malliga Sundari S., Nithyadevi N., "Magnetoconvection in an enclosure with partially active vertical walls", Int. J. of Heat and Mass Transfer, 51(2008) 1946–1954.
[7] Kakarantzas S.C., Sarris I.E., Grecos A.P., Vlachos N.S., "Magnetohydrodynamic natural convection in a vertical cylindrical cavity with sinusoidal upper wall temperature", Int. J. of Heat and Mass Transfer 52, (2009) 250–259
[8] Pirmohammadi M., Ghassemi M. and Hamedi M., "Effect of Inclination Angle on Magneto-Convection inside a Tilted Enclosure", IEEE Transactions on magnetic, Vol... 46, No. 9, (2010), SEPTEMBER
[9] Singh N. P. And Ajay Kumar Singh, "MHD Free Convection and Mass Transfer Flow Past a Flat Plate" the Arabian Journal for Science and Engineering, 32 (2003) number 1A
[10] Herman B., "Magneto hydrodynamic Flow in Ducts", The MIT Cambridge, Massachusetts, and London, England ((1978).
[11] Patanker, S. V., "Numerical Heat Transfer and Fluid Flow", Series In Computational Methods, McGraw-Hill, 1st Edition (1980).
[12] Schwab, T. H., and De Witt, K. J., "Numerical Investigation of Free Convection between Two Vertical Coaxial Cylinders", AICHE J., 16 (1970) 1005-1010.